Mathematics

https://www.aimspress.com/journal/Math

AIMS Mathematics, 10(4): 8203–8219.
DOI:10.3934/math.2025377
Received: 11 November 2024
Revised: 24 March 2025
Accepted: 01 April 2025
Published: 10 April 2025

Research article

Virtual element method for the Laplacian eigenvalue problem with Neumann boundary conditions

Junchi Ma*, **Lin Chen and Xinbo Cheng**

School of Mathematics, Liaoning Normal University, Dalian, China

* **Correspondence:** Email: majch@lnnu.edu.cn.

Abstract: The Laplacian eigenvalue problem is fundamental to the free vibration problem. The finite element method (FEM) is a classical numerical method for solving eigenvalue problems. However, for some complex problems, the flexibility of mesh generation in the FEM is not strong. The virtual element method (VEM), an extension of the FEM to polygonal meshes, offers more flexibility in mesh generation and has significant advantages when dealing with complex regions with high regularity. Additionally, the VEM does not require the explicit expression of basis functions, which simplifies the computational process. In this paper, we use the VEM to solve the Laplacian eigenvalue problem with Neumann boundary conditions. Considering standard assumptions on polygonal meshes, the source problem of the Laplacian eigenvalue problem in variational form by defining the solution operator is obtained. We then construct the virtual element space and the degrees of freedom to define the appropriate projection operator. To approximate the exact solutions, we construct discrete bilinear form and right-hand side. Furthermore, we apply the spectral approximation theory to prove the error estimates of the eigenvalues. To support the convergence analysis, a series of numerical examples is reported. For the Laplacian eigenvalue problem with Neumann boundary conditions on a square domain, experiments demonstrate the convergence behavior of approximate solutions and extrapolated values. The results indicate that the errors of the eigenvalues are converged with the refinement of the grid. Numerical experiments also verify the effectiveness of the theoretical analysis in solving eigenvalue problems under different meshes.

Keywords: virtual element method; Laplacian eigenvalue problem; Neumann boundary; spectral approximation; error estimates
Mathematics Subject Classification: 65N25, 65N30

1. Introduction

The eigenvalue problems arising from partial differential equations have become an essential field in engineering application and mathematical theory. The finite element method (FEM) [1, 2] is an important numerical method to solve the eigenvalue problems. Its outstanding advantage is that it can solve the partial differential equations in complex regions. At the same time, it is easy to implement on the computer. However, the FEM also has some limitations; it is unsuitable for some complex problems, and the flexibility of mesh generation is not strong. Therefore, the virtual element method (VEM) [3, 4] was introduced as the extension of the FEM to polygonal meshes. The mesh generation of this method is flexible, which can be a general polygon or polyhedron mesh. This method also has significant advantages when dealing with complex regions with high regularity. In addition, the VEM does not need to explicitly express the basis function, which makes the computational process easier to implement.

Actually, in recent times the VEM has been used to deal with a large range of eigenvalue problems, such as the Steklov eigenvalue problem [5, 6], the Laplacian eigenvalue problem [7, 8], the linear elasticity eigenvalue problem [9], the acoustic vibration problem [10], the buckling problem of the Kirchhoff plate [11, 12], and the transmission eigenvalue problem [13–15]. In this paper, we study the use of VEM for the approximate solution of the Laplacian eigenvalue problem with Neumann boundary conditions.

The Laplacian eigenvalue problem is a significant problem in the field of eigenvalues, which is regarded as the foundation for solving many problems in mathematics and engineering. For example, the so-called acoustic vibration problem, namely, to compute the vibration modes and the natural frequencies of an inviscid compressible fluid within a rigid cavity. The virtual element spectral approximation of the coupled systems involving the fluid-structure occurs. A simple formulation can be obtained by using the pressure variation, which leads to an eigenvalue problem involving the Laplace operator; specifically, the problem is given by the equation $\int \operatorname{div} u \operatorname{div} v = \lambda \int uv$. In addition, by expanding the Laplacian eigenvalue equation to the fourth-order equation, the vibration and buckling problems of Kirchhoff plates can be obtained as $\Delta^2 u = -\lambda \Delta u$.

Kirchhoff plate problems play an important role in the mechanical design of structures such as bridges, automobiles, and airplanes. Other versions of the Laplacian eigenvalue problem include p- and hp-versions of the VEM for elliptic eigenvalue problems [16], advection-diffusion problems [17, 18], and transmission problems [13–15].

In the two-dimensional domain, the Laplacian eigenvalue problem with Dirichlet boundary conditions is called the vibration problem of the membrane, which has been studied by many references. If boundary conditions are rewritten as Neumann boundary conditions, it is called the free vibration of the thin film. In this paper, we discuss solving the Laplacian eigenvalue problem with Neumann boundary conditions based on the VEM. We approximate the exact solution of the eigenvalue problem using the VEM, and based on the spectral approximation theory for compact operators, we derive optimal error estimates for the VEM approximation of eigenvalue problems. The validity of the theoretical analysis is verified by a set of numerical experiments.

The paper is organized as follows: We are devoted to the Laplacian eigenvalue problem with Neumann boundary conditions and the theory for the solution operator in Section 2. We obtain the source problem of the variational form and the related error estimates, construct in Section 3 the virtual element spaces and the degrees of freedom, and define appropriate the H^1 projection operator and the L^2 projection operator. In Section 4, the corresponding discrete forms are obtained by constructing a bilinear form and a right-hand side. Section 5 applies the spectral approximation for compact operators with the corresponding estimates of the space gap to obtain error estimates of the eigenvalues. Finally, we report a set of numerical tests to verify the theoretical analysis in Section 6 and draw the conclusions.

2. The model of the Laplace eigenvalue problem

Let Ω be a bounded, open, polygonal domain in $\mathbb{R}^2$ with Lipschitz continuous boundary Γ. We adopt the usual notation $\|\cdot\|_s$ and $|\cdot|_s$ for norm and seminorm in Sobolev space $H^s(\Omega)$. Similarly, $\|\cdot\|_0$ denotes the norm in Sobolev space $L^2(\Omega)$.

We are interested in the Laplace eigenvalue problem with Neumann boundary conditions; the free vibration problem of the thin film is stated as follows:

$$\begin{cases} -\Delta\omega + \beta\omega = \lambda\omega, & \text{in } \Omega, \\ \frac{\partial\omega}{\partial \boldsymbol{n}} = 0, & \text{on } \Gamma, \end{cases} \tag{2.1}$$

where $\lambda, \beta \in \mathbb{R}, \omega \in H^1(\Omega)$, and $\|\omega\|_0 = 1$, $\boldsymbol{n}$ is the unit normal vector to Γ.

Multiplying (2.1) by v and integrating over Ω, the variational formulation of problem (2.1) reads as follows: find $(\lambda, \omega) \in \mathbb{R} \times H^1(\Omega)$ with $\|\omega\|_0 = 1$ satisfying

$$a(\omega, v) = \lambda b(\omega, v), \quad \forall v \in H^1(\Omega), \tag{2.2}$$

where $a(\omega, v) = \int_\Omega (\nabla\omega \cdot \nabla v + \beta\omega v)\mathrm{d}x$ and $b(\omega, v) = \int_\Omega \omega v \mathrm{d}x$.

The source problem associated with problem (2.2) reads: given $f \in L^2(\Omega)$, find $u \in H^1(\Omega)$ such that

$$a(u, v) = b(f, v), \quad \forall v \in H^1(\Omega), \tag{2.3}$$

where the bilinear form $a(\cdot, \cdot)$ satisfy the Lax-Milgram theorem (see [19]), then there exists M independent of u and v, α independent of v, since

$$|a(u, v)| \leq M\|u\|_1\|v\|_1, \quad a(v, v) \geq \alpha\|v\|_1^2, \quad \forall u, v \in H^1(\Omega).$$

It is also well known that the variational form (2.2) has a unique solution u.

Let Ω be a bounded polygonal domain with the maximum interior angle ω ($\omega < 2\pi$). When $\omega < \pi$, let $r = 1$; when $\omega > \pi$, let $r < \frac{\pi}{\omega} - \varepsilon$ (for any $\varepsilon > 0$). Then the constant r belongs to $\left(\frac{1}{2}, 1\right]$ depends only on Ω. Hence, we have the following theorem.

Theorem 2.1. *[20] If $f \in L^2(\Omega)$, the solution $u \in H^{1+r}(\Omega)$ satisfied*

$$\|u\|_{1+r} \leq C\|f\|_0,$$

where C is a positive constant.

3. Virtual element spaces and degrees of freedom

In this section, we briefly recall the core idea of the VEM. Let $\{\mathcal{T}_h\}_h$ be a sequence of decompositions of Ω into polygons E. For each element $E \in \mathcal{T}_h$, ∂E denotes the boundary of element E, and x_E denotes the barycenter of E. As usual, h_E will also denote the diameter of the element E and h as the maximum of such diameters of all the elements in $\mathcal{T}_h$. Similarly, for each edge $e \in \partial E$, h_e is the length of e. For the moment we just assume that for all meshes $\mathcal{T}_h$, there exists a positive constant β for each element $E \in \mathcal{T}_h$ and every edge $e \in \partial E$ such that

- A1: the ratio between the shortest edge and the diameter h_E of E is larger than β, that is, $h_e \geq \beta h_E$.
- A2: E is star-shaped with respect to a disk with radius greater than βh_E.

Following Beirão da Veiga [3,21], for every integer $k \geq 1$, $\mathbb{P}_k$ is the space of polynomials of degree at most equal to k. A preliminary local space is defined by

$$\widetilde{V}_h^k(E) := \left\{ v \in H^1(E) : v|_{\partial E} \in C^0(\partial E), v|_e \in \mathbb{P}_k(e), \forall e \subset E, \Delta v \in \mathbb{P}_k(E) \right\}.$$

For each $v \in \widetilde{V}_h^k(E)$, define the following linear operator sets:

- L_1: The values of v at the all vertices of E;
- L_2: For $k > 1$, the values of v at $k-1$ internal points on each edge e of E;
- L_3: For $k > 1$, the values of the moments up to order $k-2$ of v in E,

$$\frac{1}{|E|} \int_E m_\alpha(x) v(x) \mathrm{d}x, \quad \forall m_\alpha \in \mathcal{M}_{k-2}(E),$$

  where $\mathcal{M}_{k-2}(E) := \left\{ \left(\frac{x - x_E}{h_E} \right)^s, |s| \leq k-2 \right\}$ and $\alpha = 1, \cdots, n_{k-2}$, n_{k-2} denotes the dimension of polynomials $\mathbb{P}_{k-2}(E)$.

From the sets of the linear operators, we construct a H^1 projection operator $\Pi_k^\nabla : \widetilde{V}_h^k(E) \to \mathbb{P}_k(E)$, it satisfies the following orthogonality conditions

$$\int_E \nabla \left(\Pi_k^\nabla v - v \right) \cdot \nabla p \, \mathrm{d}x = 0\,, \quad \forall p \in \mathbb{P}_k(E),$$

and

$$\int_{\partial E} \left(\Pi_k^\nabla v - v \right) \mathrm{d}s = 0.$$

We first refer to the context in [4]; there exists a positive constant C such that, for all sufficiently smooth function v, the following estimates are satisfied:

$$\left\| v - \Pi_k^\nabla v \right\|_{1,E} \leq C h_E^{s-1} |v|_{s,E}\,, \quad 1 \leq s \leq k+1.$$

Now define the L^2 projection operator $\Pi_k^0 : L^2(E) \to \mathbb{P}_k(E)$, satisfying the following regularity condition

$$\int_E (\Pi_k^0 v - v) p \, \mathrm{d}x = 0\,, \quad \forall p \in \mathbb{P}_k(E).$$

Similarly, as shown in [4], there exists a positive constant C such that, for all smooth enough function v, satisfied

$$\left\|v - \Pi_k^0 v\right\|_{m,E} \leq C h_E^{s-m} |v|_{s,E}, \quad m = 0 \text{ or } 1,\ 1 \leq s \leq k+1.$$

The local virtual element space is introduced by

$$V_h^k(E) := \left\{ v \in \widetilde{V}_h^k(E) : \int_E vp \,\mathrm{d}x = \int_E (\Pi_k^\nabla v) p \,\mathrm{d}x, \forall p \in (\mathbb{P}_k/\mathbb{P}_{k-2}(E)) \right\},$$

where $(\mathbb{P}_k/\mathbb{P}_{k-2}(E))$ denotes the space of polynomials in $\mathbb{P}_k(E)$ that are $L^2(E)$ orthogonal to all polynomials in $\mathbb{P}_{k-2}(E)$. The corresponding global virtual element space is

$$V_h^k := \{v \in H^1(\Omega) : v|_E \in V_h^k(E), \forall E \in \mathcal{T}_h\}.$$

Using the theory in [19,22], we can verify that $L_1 - L_3$ is the degrees of freedom of space V_h^k.

3.1. Virtual element discretization

Since we will mostly work on the element E, the discrete bilinear forms $a_h(\cdot,\cdot)$ and $b_h(\cdot,\cdot)$ are written separately as the sum of local contributions $a_h^E(\cdot,\cdot)$ and $b_h^E(\cdot,\cdot)$, that is

$$a_h(\cdot,\cdot) = \sum_{E\in\mathcal{T}_h} a_h^E(\cdot,\cdot), \quad b_h(\cdot,\cdot) = \sum_{E\in\mathcal{T}_h} b_h^E(\cdot,\cdot).$$

The corresponding discrete forms of the variational problem (2.3) reads: find $u_h \in V_h^k$ such that

$$a_h(u_h, v_h) = b_h(f, v_h), \quad \forall v_h \in V_h^k. \tag{3.1}$$

First of all, the discrete bilinear forms are required to be similar to the continuous ones, namely

$$a_h^E(v_h, v_h) \approx a^E(v_h, v_h), \quad b_h^E(v_h, v_h) \approx b^E(v_h, v_h).$$

In general, the continuous forms $a(\cdot,\cdot)$ and $b(\cdot,\cdot)$ are not computable on the basis functions, except for those which are polynomials. The projection operator $\Pi_k^\nabla : V_h^k(E) \to \mathbb{P}_k(E)$, for $u_h, v_h \in V_h^k(E)$, the discrete bilinear form as

$$a_h^E(u_h, v_h) = a^E\left(\Pi_k^\nabla u_h, \Pi_k^\nabla v_h\right) + S_a^E\left(\left(I - \Pi_k^\nabla\right) u_h, \left(I - \Pi_k^\nabla\right) v_h\right), \tag{3.2}$$

where $S_a^E(\cdot,\cdot)$ is a symmetric positive definite bilinear form defined on $V_h^k(E) \times V_h^k(E)$ scaling like $a^E(\cdot,\cdot)$, there exist two positive constants c_0 and c_1, such that

$$c_0 a^E(v_h, v_h) \leq S_a^E(v_h, v_h) \leq c_1 a^E(v_h, v_h), \tag{3.3}$$

for all $v_h \in V_h^k(E)$ with $\Pi_k^\nabla v_h = 0$.

We point out that (3.2) imitates the following identity:

$$a^E(u_h, v_h) = a^E\left(\Pi_k^\nabla u_h, \Pi_k^\nabla v_h\right) + a^E\left(\left(I - \Pi_k^\nabla\right) u_h, \left(I - \Pi_k^\nabla\right) v_h\right). \tag{3.4}$$

For proper choices of $S_a^E(\cdot,\cdot)$, it turns out that $a_h^E(\cdot,\cdot)$ fulfils the following important properties for all E.

Lemma 3.1. *For all $E \in \mathcal{T}_h$,*

- *Consistency: for all $v_h \in V_h^k(E)$, $p_k \in \mathbb{P}_k(E)$, it holds*

$$a_h^E(p_k, v_h) = a^E(p_k, v_h).$$

- *Stability: there exists two positive constants, α_* and α^* independent of h with $0 < \alpha_* \le \alpha^*$ such that, for all $v_h \in V_h^k(E)$,*

$$\alpha_* a^E(v_h, v_h) \le a_h^E(v_h, v_h) \le \alpha^* a^E(v_h, v_h).$$

Proof. According to the orthogonality condition of the H^1 projection operator, for all $p_k \in \mathbb{P}_k(E)$, $v_h \in V_h^k(E)$, the factors $(I - \Pi_k^\nabla)p_k$ and $(I - \Pi_k^\nabla)v_h$ satisfy the orthogonality; it holds

$$S_a^E\left((I - \Pi_k^\nabla)p_k, (I - \Pi_k^\nabla)v_h\right) = 0.$$

This important property of the H^1 projection operator plays a crucial role in the properties connecting the continuous function space and the discrete function space. According to (3.2), this could be done as follows:

$$a_h^E(p_k, v_h) = a^E(\Pi_k^\nabla p_k, \Pi_k^\nabla v_h) = a^E(p_k, v_h).$$

The above conclusion indicates that the discrete bilinear form a_h^E under the action of the H^1 projection operator is equal to the continuous bilinear form a^E, which directly acts on the original function. We conclude the proof of consistency.

Following from (3.2)–(3.4), we obtain

$$\begin{aligned}
a_h^E(v_h, v_h) =& a^E(\Pi_k^\nabla v_h, \Pi_k^\nabla v_h) + S_a^E\left((I - \Pi_k^\nabla)v_h, (I - \Pi_k^\nabla)v_h\right) \\
\le& a^E(\Pi_k^\nabla v_h, \Pi_k^\nabla v_h) + c_1 a^E((I - \Pi_k^\nabla)v_h, (I - \Pi_k^\nabla)v_h) \\
\le& \max\{1, c_1\}\left[a^E(\Pi_k^\nabla v_h, \Pi_k^\nabla v_h) + a^E((I - \Pi_k^\nabla)v_h, (I - \Pi_k^\nabla)v_h)\right] \\
=& \alpha^* a^E(v_h, v_h).
\end{aligned}$$

Similarly

$$a_h^E(v_h, v_h) \ge \min\{1, c_0\}\left[a^E(\Pi_k^\nabla v_h, \Pi_k^\nabla v_h) + a^E((I - \Pi_k^\nabla)v_h, (I - \Pi_k^\nabla)v_h)\right] = \alpha_* a^E(v_h, v_h).$$

The proof is complete. □

Now use the classical Scott-Dupont theorem in [23]; there are the following propositions.

Proposition 3.1. *There exists a positive constant C, depending only on the polynomial degree k and the shape regularity r, such that for every s with $1 \le s \le k + 1$ and for every $v \in H^s(E)$, there exists a $v_\pi \in \mathbb{P}_k(E)$ such that*

$$\|v - v_\pi\|_{0,E} + h_E |v - v_\pi|_{1,E} \le C h_E^s |v|_{s,E},$$

notice that v_π by v piecewise polynomial approximation.

Proposition 3.2. *There exists a positive constant C, depending only on the polynomial degree k and the shape regularity r, such that for every s with $2 \leq s \leq k+1$, for every h and for every $v \in H^s(E)$, there exists a $v_I \in V_h^k$ such that*

$$\|v - v_I\|_0 + h_E |v - v_I|_1 \leq C h_E^s |v|_s$$

notice that v_I by v interpolation approximation.

Dealing with the right-hand side of the discrete variational form (3.1), according to the L^2 projection operator defined in Section 3, for all elements $E \in \mathcal{T}_h$,

$$b^E(\Pi_k^0 f, p_k) = b^E(f, p_k), \quad \forall p_k \in \mathbb{P}_k(E).$$

This projection operator is computable starting from the degrees of freedom as well. Thus, for all elements $E \in \mathcal{T}_h$ such that

$$b_h^E(f, v_h) = b^E(\Pi_k^0 f, v_h), \quad \forall v_h \in V_h^k(E).$$

Theorem 3.1. *[3] Let u be the solution of problem (2.3), and let $u_h \in V_h^k$ be the solution of discrete problem (3.1); for every approximation $u_I \in V_h^k$ of u and for every approximation $u_\pi \in \mathbb{P}_k$ of u, then*

$$\|u - u_h\|_1 \leq C\left(|u - u_I|_1 + |u - u_\pi|_{1,h} + \sup_{v_h \in V_h^k} \frac{|b(f, v_h) - b_h(f, v_h)|}{|v_h|_1}\right),$$

where C is a constant independent of h, $u_I \in V_h^k$ and $u_\pi \in \mathbb{P}_k$ are defined by Propositions 3.1 and 3.2, respectively.

By applying [21], if $f \in L^2(\Omega)$, the error converges to zero depending on the regularity of the solution u,

$$\|u - u_h\|_1 \leq C\left(h\|f\|_0 + h^r |u|_{1+r}\right) \leq C h^{\min(1,t)} \|f\|_0,$$

where $t = \min(k, r)$ with k the polynomial degree and r the regularity index of the solution u.

The discrete eigenvalue problem of (2.2) is given by: find $(\lambda_h, \omega_h) \in \mathbb{R} \times V_h^k$ such that

$$a_h(\omega_h, v_h) = \lambda_h b_h(\omega_h, v_h), \quad \forall v_h \in V_h^k. \tag{3.5}$$

It is then natural to add a stability term as

$$b_h^E(\omega_h, v_h) = b^E\left(\Pi_k^0 \omega_h, \Pi_k^0 v_h\right) + S_b^E\left(\left(I - \Pi_k^0\right)\omega_h, \left(I - \Pi_k^0\right) v_h\right), \tag{3.6}$$

where $\omega_h, v_h \in V_h^k(E)$, $S_b^E(\cdot,\cdot)$ is a symmetric positive definite bilinear form defined on $V_h^k(E) \times V_h^k(E)$, that is there exists two positive constants $\widetilde{c}_0$ and $\widetilde{c}_1$, for every $v_h \in V_h^k(E)$, satisfying

$$\widetilde{c}_0 b^E(v_h, v_h) \leq S_b^E(v_h, v_h) \leq \widetilde{c}_1 b^E(v_h, v_h).$$

4. Error estimates

Theorem 4.1. *Given $f \in L^2(\Omega)$, let $u \in H^1(\Omega)$ be the solution to problem (2.3) and $u_h \in V_h^k$ be the solution to problem (3.1), such that*

$$\|u-u_h\|_0 \le Ch^r\left(|u-u_I|_1 + |u-u_\pi|_{1,h} + \left\|f-\Pi_k^0 f\right\|_0\right),$$

where C is a positive constant independent of h.

Proof. Using a duality argument and denote by $\varphi \in H^1(\Omega)$ the solution to

$$a(v,\varphi) = b(v, u-u_h), \quad \forall v \in H^1(\Omega). \tag{4.1}$$

Since $u-u_h \in L^2(\Omega)$, then for $\varphi \in H^{1+r}(\Omega)$,

$$\|\varphi\|_{1+r} \le C\,\|u-u_h\|_0 .$$

Let $\varphi_I \in V_h^k$ be the interpolant of φ; by Proposition 3.2, then for $r \in (\frac{1}{2}, 1]$, it holds

$$\|\varphi-\varphi_I\|_0 + h\,|\varphi-\varphi_I|_1 \le Ch^{1+r}\,|\varphi|_{1+r} \le Ch^{1+r}\,\|u-u_h\|_0 . \tag{4.2}$$

We have that

$$\|u-u_h\|_0^2 = b(u-u_h, u-u_h) = a(u-u_h,\varphi) = a(u-u_h,\varphi-\varphi_I) + a(u-u_h,\varphi_I) = I + II.$$

We first estimate the term I as follows:

$$I = a(u-u_h,\varphi-\varphi_I) \le C\,|u-u_h|_1\,\|\varphi-\varphi_I\|_1 \le Ch^r\,|u-u_h|_1\,\|u-u_h\|_0 .$$

Then

$$\begin{aligned} II = a(u-u_h,\varphi_I) =& b(f,\varphi_I) - a(u_h,\varphi_I) + a_h(u_h,\varphi_I) - a_h(u_h,\varphi_I) \\ =& \left[b(f,\varphi_I) - b_h(f,\varphi_I)\right] + \left[a_h(u_h,\varphi_I) - a(u_h,\varphi_I)\right] \\ =& III + IV. \end{aligned}$$

From the above, it can be inferred that

$$III = b(f,\varphi_I) - b_h(f,\varphi_I) = \sum_{E\in\mathcal{T}_h}\left[b^E(f,\varphi_I) - b^E(\Pi_k^0 f,\Pi_k^0\varphi_I) - S_b^E((I-\Pi_k^0)f,(I-\Pi_k^0)\varphi_I)\right].$$

It holds

$$\begin{aligned} b^E(f,\varphi_I) - b^E(\Pi_k^0 f,\Pi_k^0\varphi_I) =& b^E(f-\Pi_k^0 f, \varphi_I-\Pi_k^0\varphi_I) \\ \le& \left\|f-\Pi_k^0 f\right\|_0 \left\|\varphi_I-\Pi_k^0\varphi_I\right\|_1 \\ \le& Ch^r\left\|f-\Pi_k^0 f\right\|_0 \|u-u_h\|_0 , \end{aligned}$$

and

$$\begin{aligned} S_b^E((I-\Pi_k^0)f,(I-\Pi_k^0)\varphi_I) \le& \widetilde{c}_1 b^E((I-\Pi_k^0)f,(I-\Pi_k^0)\varphi_I) \\ \le& \widetilde{c}_1\left\|(I-\Pi_k^0)f\right\|_0 \left\|(I-\Pi_k^0)\varphi_I\right\|_1 \\ \le& Ch^r\left\|f-\Pi_k^0 f\right\|_0 \|u-u_h\|_0 . \end{aligned}$$

Finally, estimating the term IV with the consistency of Lemma 3.1, we obtain

$$
\begin{aligned}
IV =& a_h(u_h, \varphi_I) - a(u_h, \varphi_I) \\
=& \sum_{E \in \mathcal{T}_h} \left[a_h^E(u_h, \varphi_I) - a^E(u_h, \varphi_I) \right] \\
=& \sum_{E \in \mathcal{T}_h} \left[a_h^E(u_h - \Pi_k^0 u, \varphi_I - \Pi_k^0 \varphi_I) - a^E(u_h - \Pi_k^0 u, \varphi_I - \Pi_k^0 \varphi_I) \right] \\
\leq& \left\| u_h - \Pi_k^0 u \right\|_1 \left\| \varphi_I - \Pi_k^0 \varphi_I \right\|_1 \\
\leq& Ch^r \left(\|u - u_h\|_1 + \left\| u - \Pi_k^0 u \right\|_1 \right) \|u - u_h\|_0 .
\end{aligned}
$$

Putting together all estimates,

$$
\begin{aligned}
\|u - u_h\|_0^2 =& I + II \\
\leq& Ch^r \, |u - u_h|_1 \, \|u - u_h\|_0 + Ch^r \left\| f - \Pi_k^0 f \right\|_0 \|u - u_h\|_0 \\
&+ Ch^r \, \|u - u_h\|_0 \left(\|u_h - u\|_1 + \left\| u - \Pi_k^0 u \right\|_1 \right) \\
=& Ch^r \, \|u - u_h\|_0 \left(\|u - u_h\|_1 + \left\| f - \Pi_k^0 f \right\|_0 + \left\| u - \Pi_k^0 u \right\|_1 \right).
\end{aligned}
$$

So

$$
\|u - u_h\|_0 \leq Ch^r \left(\|u - u_h\|_1 + \left\| f - \Pi_k^0 f \right\|_0 + \left\| u - \Pi_k^0 u \right\|_1 \right).
$$

We conclude the proof. □

Theorem 4.2. *Let T and T_h be the solution operators with problems (2.3) and (3.1), respectively. Then the following uniform convergence holds:*

$$
\|T - T_h\|_{\mathcal{L}(L^2(\Omega))} \to 0, \quad \text{as } h \to 0.
$$

Proof. Given $f \in L^2(\Omega)$, let Tf and $T_h f$ be the solutions to problems (2.3) and (3.1), respectively. Then, using the error estimates of Theorem 4.1, $u_I \in V_h^k$ and $u_\pi \in \mathbb{P}_k$ are given by Propositions 3.1 and 3.2, and the stability condition of Theorem 2.1, we obtain

$$
\|Tf - T_h f\|_0 = \|u - u_h\|_0 \leq Ch^r \left(|u - u_I|_1 + |u - u_\pi|_1 + \left\| f - \Pi_k^0 f \right\|_0 \right) \leq Ch^t \, \|f\|_0 ,
$$

where $t = \min(k, r)$, $k \geq 1$ is the order, r is the regularity index, and C is a constant independent of h.

Thus, from the definition of the operator norm, we have

$$
\|T - T_h\|_{\mathcal{L}(L^2(\Omega))} = \sup_{f \in L^2(\Omega)} \frac{\|Tf - T_h f\|_0}{\|f\|_0} \leq Ch^t,
$$

which implies the uniform convergence. □

Lemma 4.1. *[19] Let λ_i be an eigenvalue of problem (2.1), with multiplicity m (that is $\lambda_i = \cdots = \lambda_{i+m-1}$) and let E_λ be the corresponding eigenspace. The discrete eigenvalues $\lambda_{1,h}, \lambda_{2,h}, \cdots, \lambda_{m,h}$ converge to λ_i. Moreover, let $E_{\lambda,h}$ be the direct sum of the eigenspaces corresponding to the discrete eigenvalues $\lambda_{1,h}, \lambda_{2,h}, \cdots, \lambda_{m,h}$. Then, there exists a constant C independent of h such that*

$$
\delta(E_\lambda, E_{\lambda,h}) \leq C \left\| (T - T_h)|_{E_\lambda} \right\|_{\mathcal{L}(L^2(\Omega))} ,
$$

where $(T - T_h)|_{E_\lambda}$ denotes the restriction of eigenspace E_λ to $T - T_h$.

Lemma 4.2. *[19] Let $\phi_1, \cdots, \phi_m$ be a basis of the eigenspace E_λ corresponding to the eigenvalue λ_i, then, for $i = 1, \cdots, m$,*

$$\left|\lambda_i - \lambda_{h,i}\right| \leq C\left(\sum_{j,k=1}^{m}\left|b((T - T_h)\phi_k, \phi_j)\right| + \left\|(T - T_h)|_{E_\lambda}\right\|^2_{\mathcal{L}(L^2(\Omega))}\right).$$

Theorem 4.3. *Under the assumptions of Lemma 4.1, there exists a constant C such that*

$$\delta(E_\lambda, E_{\lambda,h}) \leq Ch^t,$$

where $t = \min(k, r)$, k is the polynomial degree and r is the regularity index.

Proof. The result directly stems from Theorem 4.2. Indeed,

$$\delta(E_\lambda, E_{\lambda,h}) \leq C\left\|(T - T_h)|_{E_\lambda}\right\|_{\mathcal{L}(L^2(\Omega))} = C \sup_{f\in E_\lambda, f\neq 0} \frac{\|Tf - T_h f\|_0}{\|f\|_0} \leq Ch^t.$$

We conclude the proof. □

Theorem 4.4. *Using the notation of Lemma 4.1, there exists a constant C independent of h but depending on λ such that*

$$\left|\lambda_i - \lambda_{h,i}\right| \leq Ch^{2t}, \quad i = 1, \cdots, m.$$

Proof. We apply Lemma 4.2; it remains to bound the first term. Let κ and z be the elements of E_λ. Firstly, we estimate $b((T - T_h)\kappa, z)$, for all κ and z in E_λ

$$\begin{aligned}
b\left((T - T_h)\kappa, z\right) =& a\left(Tz, (T - T_h)\kappa\right) \\
=& a\left((T - T_h)z, (T - T_h)\kappa\right) + a\left(T_h z, (T - T_h)\kappa\right) \\
=& a\left((T - T_h)z, (T - T_h)\kappa\right) + a\left(T_h z, T\kappa\right) - a\left(T_h z, T_h\kappa\right) \\
=& a\left((T - T_h)z, (T - T_h)\kappa\right) + b\left(T_h z, \kappa\right) - a\left(T_h z, T_h\kappa\right) \\
=& a\left((T - T_h)z, (T - T_h)\kappa\right) + b\left(T_h z, \kappa\right) - a_h\left(T_h z, T_h\kappa\right) + a_h\left(T_h z, T_h\kappa\right) - a\left(T_h z, T_h\kappa\right) \\
=& a\left((T - T_h)z, (T - T_h)\kappa\right) + b\left(T_h z, \kappa\right) - b_h\left(T_h z, \kappa\right) + a_h\left(T_h z, T_h\kappa\right) - a\left(T_h z, T_h\kappa\right) \\
=& I' + II' + III'.
\end{aligned}$$

We estimate separately the above three terms. It is straightforward to obtain

$$I' \leq \|(T - T_h)z\|_1 \, \|(T - T_h)\kappa\|_1 \leq Ch^{2t}.$$

In order to estimate the second term, we proceed as in (3.6) by writing it as a sum over the elements $E \in \mathcal{T}_h$,

$$\begin{aligned}
II' =& \sum_E \left[b^E\left((I - \Pi_k^0)T_h z, (I - \Pi_k^0)\kappa\right) - S_b^E\left((I - \Pi_k^0)T_h z, (I - \Pi_k^0)\kappa\right)\right] \\
\leq& C\sum_E \left\|(I - \Pi_k^0)T_h z\right\|_{0,E} \left\|(I - \Pi_k^0)\kappa\right\|_{0,E} \\
\leq& Ch^{2t}.
\end{aligned}$$

Finally,

$$\begin{aligned} III' =& \sum_E \left[a_h^E \left(T_h z - \Pi_k^0 T z, T_h \kappa - \Pi_k^0 T k \right) - a^E \left(T_h z - \Pi_k^0 T z, T_h \kappa - \Pi_k^0 T \kappa \right) \right] \\ \leq& C \sum_E \left(|T_h z - Tz|_{1,E} + \left| (I - \Pi_k^0) T z) \right|_{1,E} \right) \left(|T_h \kappa - T\kappa|_{1,E} + \left| (I - \Pi_k^0) T \kappa \right|_{1,E} \right) \\ \leq& C h^{2t}. \end{aligned}$$

Putting together all estimates, we have

$$b((T - T_h)\kappa, z) \leq C h^{2t}.$$

Combined with Theorem 4.3, the conclusion is proved. □

5. Numerical tests

In this section, we present the VEM approximation of the Laplacian eigenvalue problem with Neumann boundary conditions. Regarding the computational domain, in the test we take the square domain $\Omega \in [0, 1]^2$. On this domain, we first consider the mesh partitionings, performed in polygonal or quadrilateral decomposition. The refinement parameter N used to label each mesh is the number of elements. These successively refined mesh numbers, 20, 50, 100, and 250, are shown in Figure 1. We follow the way in literature [3] and set up $S_a^E(\cdot, \cdot)$ or $S_b^E(\cdot, \cdot)$ by defining the local degrees of freedom suitably.

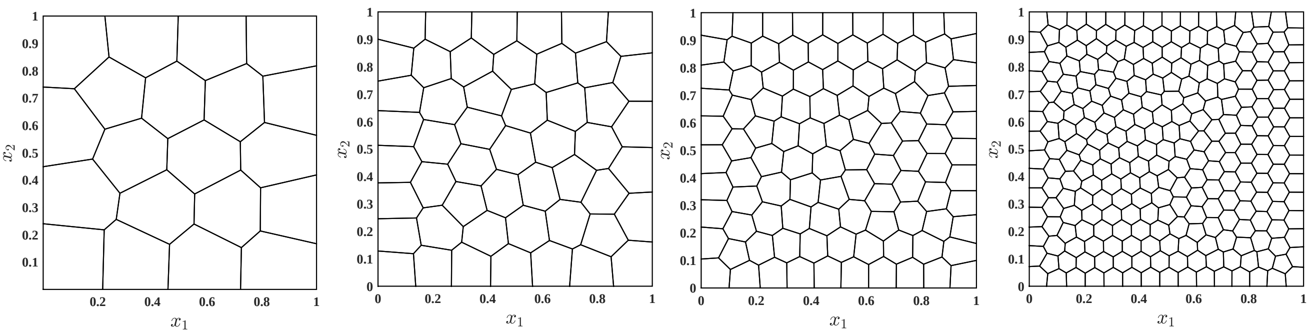

(a) $N = 20$ (b) $N = 50$ (c) $N = 100$ (d) $N = 250$

Figure 1. The polygonal meshes with different mesh numbers in square domain.

The approximate solution of the problem (2.1) is obtained, and the eigenvalues that are closer to the exact solutions, which are extrapolated from several approximate solutions by means of a least-squares fit. The approximate solutions and extrapolated values exhibit convergence behavior, with their corresponding convergence orders characterizing the speed of convergence. It can be seen that the theoretical order of convergence is only a lower bound since the actual order of convergence for each unit depends on the regularity of the corresponding partitioning shape. Therefore, the attained orders of convergence are larger than this lower bound. Table 1 presents the first six eigenvalues computed using the analyzed method, with grid numbers of 20, 50, 100, and 250, respectively. The extrapolated value of each eigenvalue is calculated, where $\lambda_{h,i}$ denotes the approximate solution of problem (2.1) and $\lambda_{\text{extr},i}$ is the corresponding extrapolated value. The last column of Table 1 contains the estimated convergence orders of each eigenvalue. The convergence order is an average value that is defined by

$$\text{Order} := \log_2 \frac{\left\|\lambda_{\text{extr},i} - \lambda_{2h,i}\right\|}{\left\|\lambda_{\text{extr},i} - \lambda_{h,i}\right\|}.$$

Table 1. The first six eigenvalues $\lambda_{h,i}(1 \le i \le 6)$ in polygonal meshes.

	$N = 20$	$N = 50$	$N = 100$	$N = 250$	$\lambda_{\text{extr},i}$	Order
$\lambda_{h,1}$	3.1504	3.4887	3.4727	3. 4695	3.4684	1.87
$\lambda_{h,2}$	3.2780	3.5243	3.4736	3.4700	3.4519	1.09
$\lambda_{h,3}$	3.3117	3.5390	3.4812	3.4849	3.4669	1.04
$\lambda_{h,4}$	3.3504	3.5605	3.5487	3.5061	3.4919	1.11
$\lambda_{h,5}$	3.4749	3.5980	3.5682	3.5473	3.5421	1.07
$\lambda_{h,6}$	3.7033	3.6212	3.6507	3.5619	3.7125	1.01

In this case, to have a view of the convergence rate, the absolute error and relative error are given as shown in Figure 2. For the first six eigenvalues, the absolute errors as the refinement parameter are seen on the left-hand side of Figure 2. The relative errors are shown on the right-hand side, where the horizontal coordinates represent the polygonal meshes for N= 20, 50, 100, and 250. The absolute errors and relative errors for the first six eigenvalues and the extrapolated values can be found; it can be found that the errors of the eigenvalues converge with the refinement of the grid. The slopes of the folded lines in the figures indicate the convergence orders of eigenvalues. The slopes in the figures are consistent with the convergence order obtained. Here, the absolute error $Err(\lambda_{h,i})$ and the relative error $err(\lambda_{h,i})$ are defined as, for $i = 1, \cdots, 6$,

$$Err(\lambda_{h,i}) := \left\|\lambda_{\text{extr},i} - \lambda_{h,i}\right\|, \quad err(\lambda_{h,i}) := \frac{\left\|\lambda_{\text{extr},i} - \lambda_{h,i}\right\|}{\left\|\lambda_{\text{extr},i}\right\|}.$$

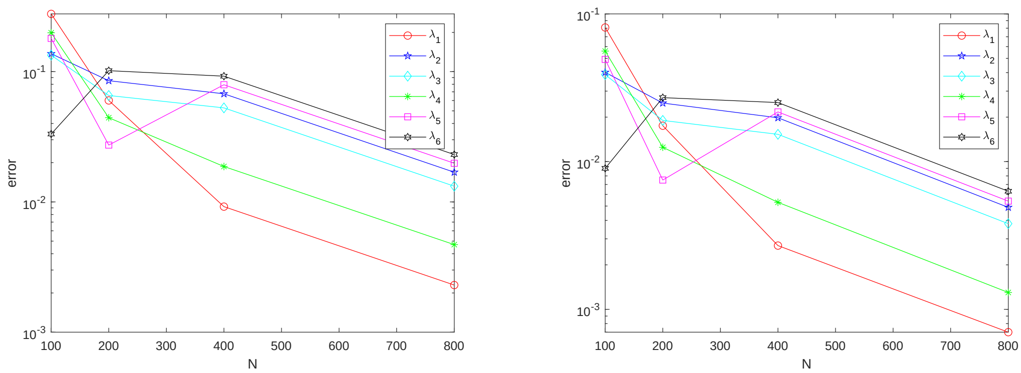

(a) Absolute error (b) Relative error

Figure 2. Absolute error and relative error distribution obtained in polygonal meshes.

Next, consider the square meshes of the square domain $\Omega \in [0, 1]^2$, taking the refinement parameter N is 16, 64, 256, and 400, respectively, as shown in Figure 3.

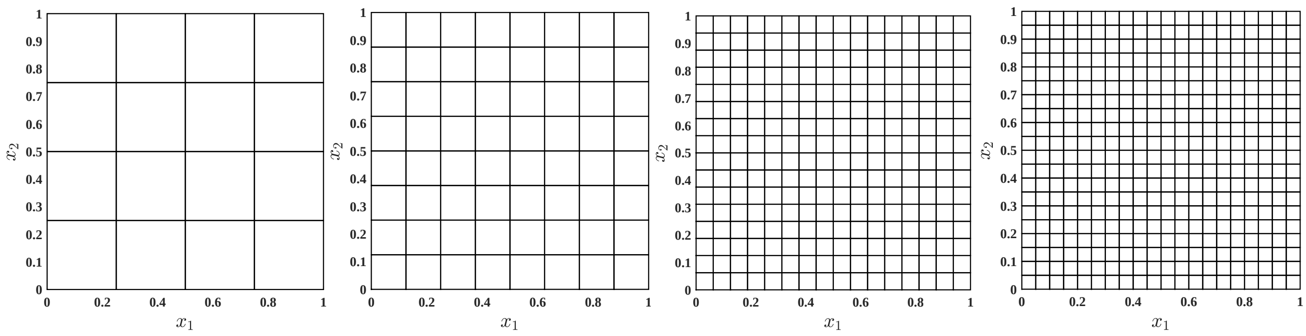

(*a*) $N = 16$ (*b*) $N = 64$ (*c*) $N = 256$ (*d*) $N = 400$

Figure 3. The square meshes with different mesh numbers in square domain.

The first six approximate eigenvalues of the problem (2.1) are obtained through numerical experiments. Since the structure of meshes is different, the eigenvalues corresponding to different shapes are different. For the same number of meshes, the eigenvalues of different element structures are still different. In Table 2, we present the obtained numerical results by the VEM using square meshes, and the corresponding extrapolated values are calculated. We can see that $\lambda_{h,4}$ equals to $\lambda_{h,5}$ in Table 2, so the eigenvalue is double. We still calculate the convergence orders according to the above formula. The convergence orders are greater than 1; thus, these experiments confirm the corresponding results of the theoretical analysis. Similarly, in order to check the convergence rate of the problem (2.1), the absolute error and relative error are given as Figure 4. The errors and convergence orders of the fourth and the fifth eigenvalues are the same, and others are not much different.

Table 2. The first six eigenvalues $\lambda_{h,i}$ $(1 \leq i \leq 6)$ in square meshes.

	$N = 16$	$N = 64$	$N = 256$	$N = 400$	$\lambda_{\text{extr},i}$	Order
$\lambda_{h,1}$	3.2557	3.9333	3.9945	3.9977	4.0192	1.72
$\lambda_{h,2}$	3.6559	3.9566	3.9968	3.9987	4.0127	1.56
$\lambda_{h,3}$	3.6614	3.9577	3.9968	3.9987	4.0124	1.55
$\lambda_{h,4}$	3.7774	3.9790	3.9986	3.9994	4.0062	1.69
$\lambda_{h,5}$	3.7774	3.9790	3.9986	3.9994	4.0062	1.69
$\lambda_{h,6}$	3.9281	3.9944	3.9996	3.9998	4.0016	1.78

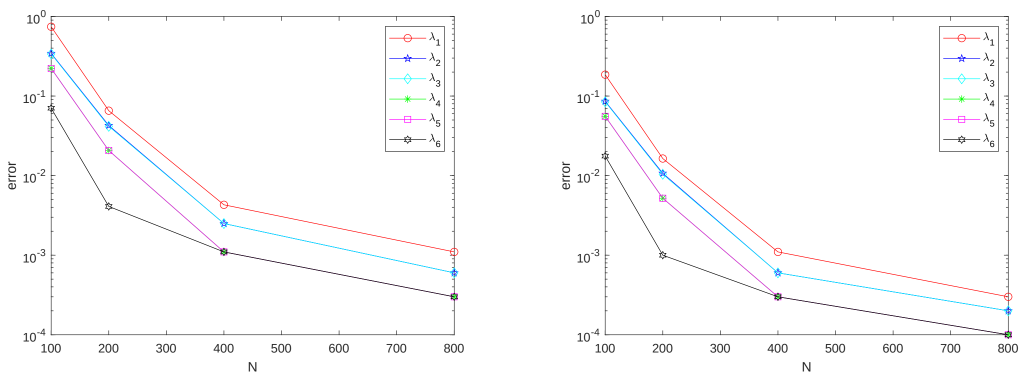

(*a*) Absolute error (*b*) Relative error

Figure 4. Absolute error and relative error distribution obtained in square meshes.

The considered region is $[0, 8] \times [-2, 2]$. The elements are divided into polygons and squares separately. The refinement parameter N is 18, 72, 288, and 1152, respectively. In Tables 3 and 4, we present the eigenvalues by the VEM using polygonal meshes and square meshes. The corresponding extrapolated values and convergence orders are shown in the last two columns of Tables 3 and 4. It can be seen that the convergence order for the same parameter N depends on the regularity of the corresponding partitioning shape. The absolute and relative errors of polygonal and square meshes are given in Figures 5 and 6.

Table 3. The first six eigenvalues $\lambda_{h,i}(1 \le i \le 6)$ in polygonal meshes.

	$N = 18$	$N = 72$	$N = 288$	$N = 1152$	$\lambda_{\text{extr},i}$	Order
$\lambda_{h,1}$	3.5380	4.3916	4.4263	4.5857	4.6388	1.46
$\lambda_{h,2}$	3.7461	4.4232	4.4542	4.6013	4.6503	1.40
$\lambda_{h,3}$	3.9322	4.4938	4.4903	4.6068	4.6456	1.40
$\lambda_{h,4}$	3.9369	4.5326	4.5524	4.6589	4.6944	1.47
$\lambda_{h,5}$	4.3670	4.6145	4.7391	4.6924	4.6768	1.44
$\lambda_{h,6}$	4.5343	5.0401	4.7716	4.8210	4.8375	1.40

Table 4. The first six eigenvalues $\lambda_{h,i}(1 \le i \le 6)$ in square meshes.

	$N = 18$	$N = 72$	$N = 288$	$N = 1152$	$\lambda_{\text{extr},i}$	Order
$\lambda_{h,1}$	4.1331	4.9580	5.2579	5.3505	5.3814	1.78
$\lambda_{h,2}$	4.2682	5.0011	5.2758	5.3561	5.3829	1.79
$\lambda_{h,3}$	4.3123	5.0097	5.2789	5.3568	5.3828	1.79
$\lambda_{h,4}$	4.4065	5.0450	5.2847	5.3576	5.3819	1.78
$\lambda_{h,5}$	4.5468	5.0995	5.3009	5.3619	5.3822	1.79
$\lambda_{h,6}$	4.8631	5.2255	5.3411	5.3733	5.3840	1.87

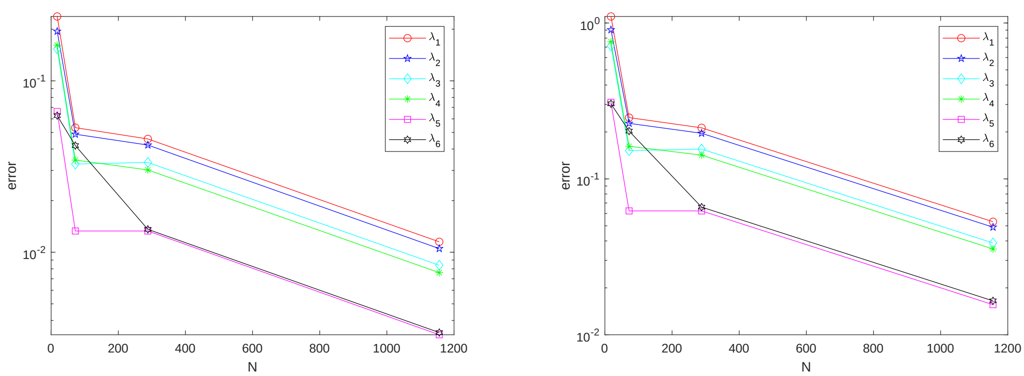

(a) Absolute error (b) Relative error

Figure 5. Absolute error and relative error distribution obtained in polygonal meshes.

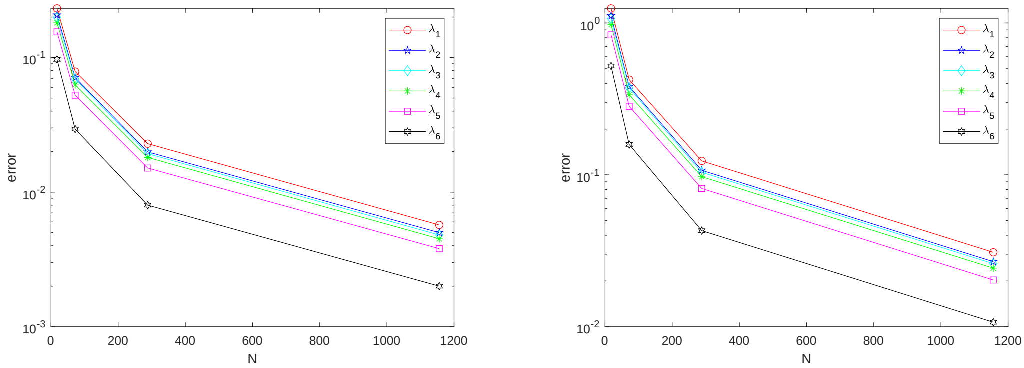

(*a*) Absolute error (*b*) Relative error

Figure 6. Absolute error and relative error distribution obtained in square meshes.

According to the convergence orders of the first six eigenvalues in Tables 1–4, it is found that the numerical results and the corresponding extrapolated value are close enough. Through Figures 2 and 4–6, the absolute error and relative error of the first six eigenvalues show an obvious convergence trend. The convergence rate is in accordance with the convergence order in the corresponding conclusion. The effectiveness of the VEM for solving the Laplacian eigenvalue problem with Neumann boundary conditions can be verified.

6. Conclusions

We consider the application of the virtual element method to solve the Laplacian eigenvalue problem with Neumann boundary conditions. Our theoretical investigation shows that the numerical algorithm provides the correct spectral approximation. And the error estimates of the eigenvalues and eigenvectors are given according to the spectral approximation theory of the compact operator. Representative numerical experiments confirm the theoretical prediction, and the validity and feasibility of the VEM are verified by numerical experiments to solve the eigenvalue problems in the domain with different meshes.

Notice that some negative aspects of the current VEM should be considered. For the three-dimensional eigenvalue problems, there are few numerical results of the VEM, which restricted its application in practice. Therefore, the VEM can be applied to other more practical eigenvalue problems, such as the stream eigenvalue problem, the transmission eigenvalue problem, and the electromagnetic eigenvalue problem, to solve more practical problems. The upcoming article will investigate the corresponding theory.

Author contributions

Junchi Ma and Lin Chen: Methodology, writing the original draft; Xinbo Cheng: Sorting data. All authors have read the manuscript.

Use of Generative-AI tools declaration

The authors declare they have not used Artificial Intelligence (AI) tools in the creation of this article.

Acknowledgments

This work was supported by the Basic Research Projects of the Liaoning Provincial Department of Education (No. JYTMS20231045).

Conflict of interest

All authors declare no conflicts of interest in this paper.

References

1. S. C. Brenner, L. Ridgway Scott, *The mathematical theory of finite element methods*, New York: Springer, 2008. https://doi.org/10.1007/978-0-387-75934-0
2. P. F. Zhu, K. Liu, Numerical investigation of convergence in the L^∞ norm for modified SGFEM applied to elliptic interface problems, *AIMS Mathematics*, **9** (2024), 31252–31273. https://doi.org/10.3934/math.20241507
3. L. Beirão da Veiga, F. Brezzi, A. Cangiani, G. Manzini, L. D. Marini, A. Russo, Basic principles of virtual element methods, *Math. Mod. Meth. Appl. S.*, **23** (2013), 199–214. https://doi.org/10.1142/S0218202512500492
4. L. Beirão da Veiga, F. Brezzi, L. D. Marini, A. Russo, Virtual element method for general second-order elliptic problems on polygonal meshes, *Math. Mod. Meth. Appl. S.*, **26** (2016), 729–750. https://doi.org/10.1142/S0218202516500160
5. D. Mora, G. Rivera, R. Rodríguez, A posteriori error estimates for a virtual element method for the Steklov eigenvalue problem, *Comput. Math. Appl.*, **74** (2017), 2172–2190. https://doi.org/10.1016/j.camwa.2017.05.016
6. G. Monzón, A virtual element method for a biharmonic Steklov eigenvalue problem, *Adv. Pure Appl. Math.*, **10** (2019), 325–337. https://doi.org/10.1515/apam-2018-0072
7. F. Gardini, G. Vacca, Virtual element method for second-order elliptic eigenvalue problems, *IMA J. Numer. Anal.*, **38** (2018), 2026–2054. https://doi.org/10.1093/imanum/drx063
8. X. Y. Wang, G. Wang, P. Yang, Novel Pareto Z-eigenvalue inclusion intervals for tensor eigenvalue complementarity problems and its applications, *AIMS Mathematics*, **9** (2024), 30214–30229. https://doi.org/10.3934/math.20241459
9. D. Mora, G. Rivera, A priori and a posteriori error estimates for a virtual element spectral analysis for the elasticity equations, *IMA J. Numer. Anal.*, **40** (2020), 322–357. https://doi.org/10.1093/imanum/dry063
10. L. Beirão da Veiga, D. Mora, G. Rivera, R. Rodríguez, A virtual element method for the acoustic vibration problem, *Numer. Math.*, **136** (2017), 725–763. https://doi.org/10.1007/s00211-016-0855-5

11. D. Mora, G. Rivera, I. Velásquez, A virtual element method for the vibration problem of Kirchhoff plates, *ESAIM: M2AN*, **52** (2018), 1437–1456. https://doi.org/10.1051/m2an/2017041

12. J. Meng, L. Q. Mei, A linear virtual element method for the Kirchhoff plate buckling problem, *Appl. Math. Lett.*, **103** (2020), 106188. https://doi.org/10.1016/j.aml.2019.106188

13. D. Mora, I. Velásquez, A virtual element method for the transmission eigenvalue problem, *Math. Mod. Meth. Appl. S.*, **28** (2018), 2803–2831. https://doi.org/10.1142/S0218202518500616

14. D. Mora, I. Velásquez, Virtual elements for the transmission eigenvalue problem on polytopal meshes, *SIAM J. Sci. Comput.*, **43** (2021), A2425–A2447. https://doi.org/10.1137/20M1347887

15. J. Meng, G. Wang, L. Mei, A lowest-order virtual element method for the Helmholtz transmission eigenvalue problem, *Calcolo*, **58** (2021), 2. https://doi.org/10.1007/s10092-020-00391-5

16. O. Čertík, F. Gardini, G. Manzini, L. Mascotto, G. Vacca, The *p*- and *hp*-versions of the virtual element method for elliptic eigenvalue problems, *Comput. Math. Appl.*, **79** (2020), 2035–2056. https://doi.org/10.1016/j.camwa.2019.10.018

17. M. F. Benedetto, S. Berrone, A. Borio, S. Pieraccini, S. Scialò, Order preserving SUPG stabilization for the virtual element formulation of advection-diffusion problems, *Comput. Method. Appl. M.*, **311** (2016), 18–40. https://doi.org/10.1016/j.cma.2016.07.043

18. S. Berrone, A. Borio, G. Manzini, SUPG stabilization for the nonconforming virtual element method for advection-diffusion-reaction equations, *Comput. Method. Appl. M.*, **340** (2018), 500–529. https://doi.org/10.1016/j.cma.2018.05.027

19. I. Babuška, J. Osborn, Eigenvalue problems, *Handbook of Numerical Analysis*, **2** (1991), 641–787. https://doi.org/10.1016/S1570-8659(05)80042-0

20. P. Grisvard, Behavior of the solutions of an elliptic boundary value problem in a polygonal or polyhedral domain, *Proceedings of the Third Symposium on the Numerical Solution of Partial Differential Equations*, 1976, 207–274. https://doi.org/10.1016/B978-0-12-358503-5.50013-0

21. B. Ahmad, A. Alsaedi, F. Brezzi, L. D. Marini, A. Russo, Equivalent projectors for virtual element methods, *Comput. Math. Appl.*, **66** (2013), 376–391. https://doi.org/10.1016/j.camwa.2013.05.015

22. J. P. Wang, X. Ye, A weak Galerkin mixed finite element method for second order elliptic problems, *Math. Comp.*, **83** (2014), 2101–2126. https://doi.org/10.1090/s0025-5718-2014-02852-4

23. A. Cangiani, F. Gardini, G. Manzini, Convergence of the mimetic finite difference method for eigenvalue problems in mixed form, *Comput. Method. Appl. M.*, **200** (2011), 1150–1160. https://doi.org/10.1016/j.cma.2010.06.011